



Review Paper

Electron Transport in Zigzag Silicon and Silicon Mono-Oxide Nanoribbons: Ab initio study

Verma Mohan L.¹ and Singh Rachna*²

¹Computational Nanoionics Research Lab, Department of Applied Physics, FET-SSGI, Shri Shankaracharya Technical Campus, Junwani, Bhilai, Chhattisgarh, India, 490020

²Department of Applied Physics, Uday Prasad Uday Government Polytechnic-Durg, Chhattisgarh, India
rachnasingh10930@gmail.com

Available online at: www.isca.in, www.isca.me

Received 25th February 2016, revised 3rd April 2016, accepted 30th April 2016

Abstract

Graphene and single layer silicon (silicene) are supposed to have excellent electronic properties. A theoretical study on zigzag silicon and silicon mono-oxide nanoribbons has been performed in honeycomb structures within the framework of density functional theory (DFT). There exist theoretical studies on mono-layer buckled silicon but not on silicon mono-oxide. In this paper we have tried to present a comparative study of the structural, electronic and transport properties of zigzag silicene nanoribbon and zigzag silicon mono-oxide nanoribbon. A first principle approach has been made for the structural optimization of silicene and silicon mono-oxide nanoribbon followed by electronic properties study viz. density of states, charge densities and finally transports properties like transmission energy and I-V characteristics prominently.

Keywords: Density functional theory, Nanoribbon, Transport properties, Density of states, Charge density, I-V Characteristics.

Introduction

As reported recently by many researchers Silicon and Germanium can also form stable honeycomb structures like carbon¹. It was also reported that on the Born-Oppenheimer surface a low-buckled or puckered geometry represents to a stable local minimum. Even in some earlier studies buckled honeycomb structure of Si was mentioned²⁻⁴. Although Si and Ge mono layers have puckered geometrical structures but their electronic band structures are similar to that of graphene. Depending on the width and orientation, Si and Ge nanoribbons exhibit interesting electronic and magnetic properties. Nanostructures of single crystal silicon exhibit a variety of applications in electronics, optoelectronics, sensing, and other areas in the form of wires, ribbons, and particles. The ribbon geometry is very important for certain devices as it provides large planar surfaces for chemical sensing and photo detection and it can fill efficiently the channel regions of transistors⁵.

In the present paper, probably for the first time, a systematic study of structural and electron transport studies on zigzag silicon mono oxide nanoribbons have been performed. The first principle study of transport properties were carried out within the framework of density-functional theory (DFT) combined with the non-equilibrium Green's function method (NEGF), as administered in the TranSiesta module (siesta-trunk-462 code)⁶. In this study we have taken silicon mono oxide nanoribbons along with conventional silicene nanoribbon. After structural

optimization of both models of nanoribbons the comparative studies have been performed for their electronic structures giving emphasis on transport properties at different biasing conditions. On the basis of this study, we have tried to investigate whether silicon monoxide could be used as a substitute for graphene in electronics industry.

Computational Aspects

The calculations are performed in all three model structures within the super cell approach with 20 atoms in each unit cell of respective structures with increasing the 5 unit cell in z-direction i.e. the structure is periodic along the z-axis. The electronic transport calculations in the scattering region and relaxation have been performed using super cells of SiOznr 12.93x2.64x23.15 and Siznr 15.09x2.23x37.44 while for the electrodes the unit-cell selected was 12.93x2.64x4.63 and 15.09x2.23x7.48 respectively. The mesh-cutoff value has been taken as 100 Ry in the calculations of self-consistent potential and total energy, the Brillouin zone is sampled by 1x1x20 special k points. To describe the exchange and correlation potential we have used the exchange correlation functional as generalized gradient approximation (GGA) in the scheme of Perdew-Burke-Eruzerhof (PBE)⁷, since the GGA is relatively more efficient to anticipate the energy gap of semiconductor than the local-density approximation (LDA)⁸. LDA is well known to estimate the fundamental band gap in insulators & semiconductors by 30-60%⁹. All atomic positions and unit cells

are optimized by adopting single zeta (SZ) basis set in the conjugate-gradient method until the atomic forces are less than 0.03 eV/ \AA^0 . The main idea of quantum transport calculations is to divide the system under investigation into three parts: two electrodes and a region in between known as scattering region.

The above model shown in Figure-1 depicts three parts mentioned above, left electrode, right electrode which are semi infinite and a central region. Central region constitutes the

scattering region where as the left and right electrodes are the extensions of it¹⁰⁻¹². In order to prevent the interaction between the two electrodes the size of scattering region has been considered of sufficient dimensions. The junction is so constructed that the periodic replicas of the Siznr are separated by nanometer range parallel to the electrode edge. Landauer-Buttiker Formula has been used to calculate the current through contact region¹³.

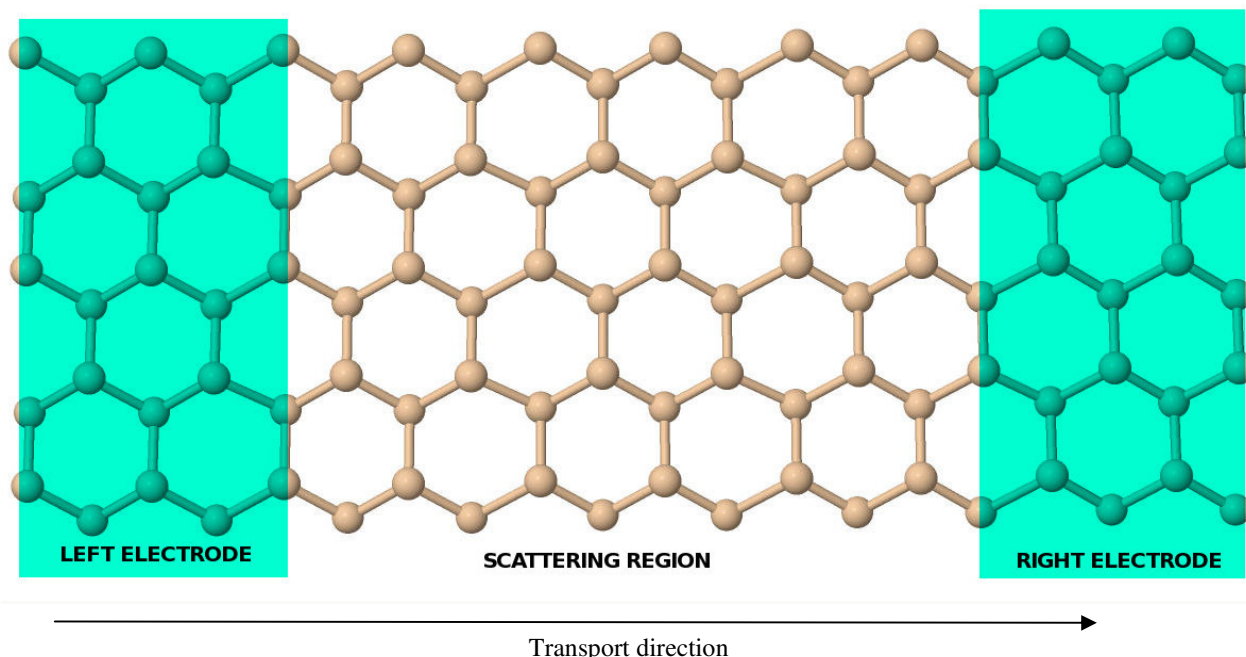


Figure-1

Schematic structure of the model device constituted by three parts: the left (L) and right (R) semi-infinite SiOznr (electrodes) and scattering region (Color online)

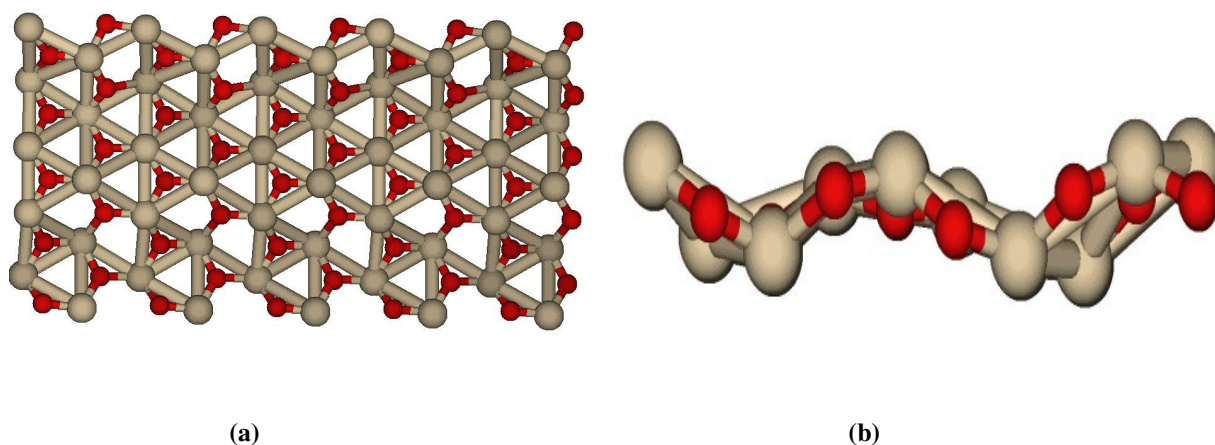


Figure-2

(a) The optimized structure of SiOznr – top view and (b) The optimized structure of SiOznr – side view in perpendicular direction to show the width of nanoribbon

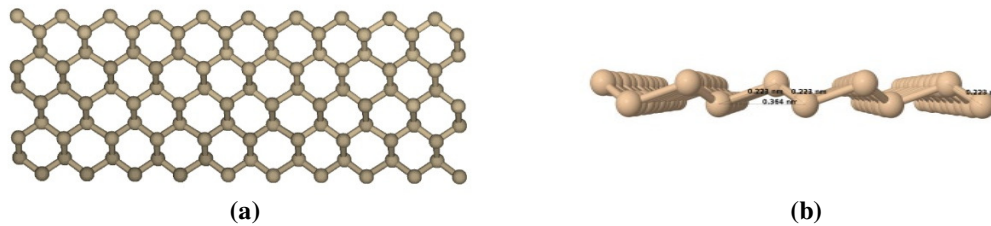


Figure-3
(a) The optimized structure of Siznr – top view and (b) The optimized structure of SiOznr – side view in perpendicular direction to show the width of nanoribbon

Table-1
Comparison of the values of bond length of Si-Si and Si-O and total energy

Configuration	Fermi energy E_F (eV)	Total energy (eV) per atom	Bond length Å^0
SiOznr	-2.09	-16.58	1.55 (Si-O) 2.88 (Si-Si)
Siznr	-5.42	-5.42	2.23 (Si-Si)

If we compare total energies we observe that SiOznr is having least total energy hence it is most stable as compared to Siznr. Moreover Fermi energy is not directly related to stability until we study its position on the DOS which is discussed in the later part of this paper.

In order to show the charge distribution of these two material models, Figure-4,5 show the charge density plots at zero bias for SiOznr, and Siznr respectively. Electron density is highest in the innermost contour (blue) and lowest in the outermost contour (red). Core zones of Si and O are blue, bonding zone is green. Figure-4 shows that electron density is concentrated around Oxygen atom and bonding between Si-O is very strong. Similarly prominent blue and green color in Figure-5 shows strong Si-Si bonding. The transport properties of SiOznr and Siznr have been studied at varying biasing voltages in the range of -1.0 V to 1.0 V in equal interval of 0.25 and discussed in next subsection.

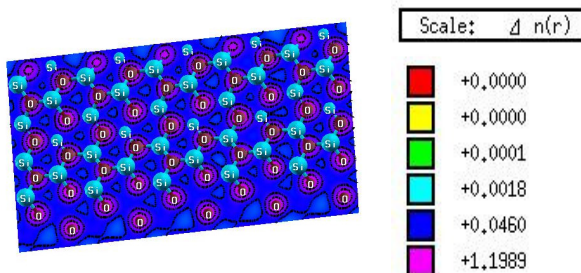


Figure-4
Charge density plots of SiOznr at zero bias and scale of charge density (Color online)

decreases with increasing bias voltage, which can be used for constructing bi-stable devices and some efficient functional components like latches, oscillators, memories¹⁴⁻¹⁵. Interestingly, the origin of NDR behavior in molecular electronics devices could involve different mechanisms¹⁶⁻¹⁷ thus, the intensity of transmission peaks decrease at high bias voltage, resulting in NDR. Figure-6 shows the I-V characteristic curve of SiOznr. As revealed from this curve of SiOznr up to 0.3 V there is no current flow with increase in bias voltage. The device is supposed to be in OFF state. After 0.3 V.

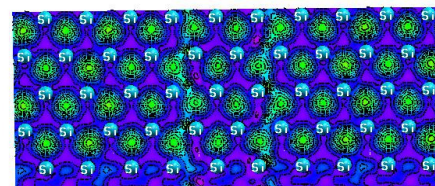


Figure-5
Charge density plots of Siznr at zero bias and scale of charge density (Color online)

Transport property analysis

Characteristics Analysis (I-V): NDR (Negative differential resistance) is a property of electrical circuits; the current

There is considerable increase in current (~4 μA). At 0.4 V there is sharp decrease in current with voltage which indicates NDR characteristics (to a small extent as at 0.75 V again there is a sharp increase in current). The strange behaviour is observed at 0.75 volt and is further being studied.

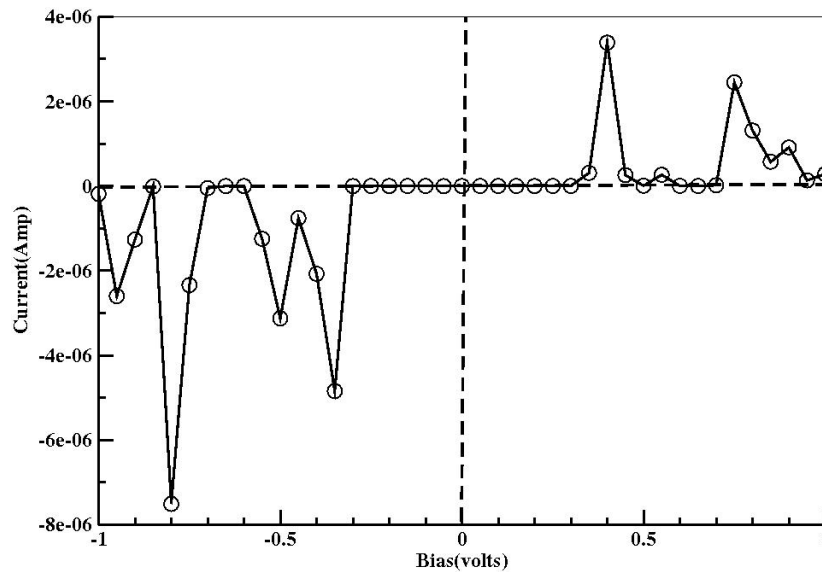


Figure-6

Characteristic Curve I-V of SiOznr showing variation of current with applied positive and negative bias

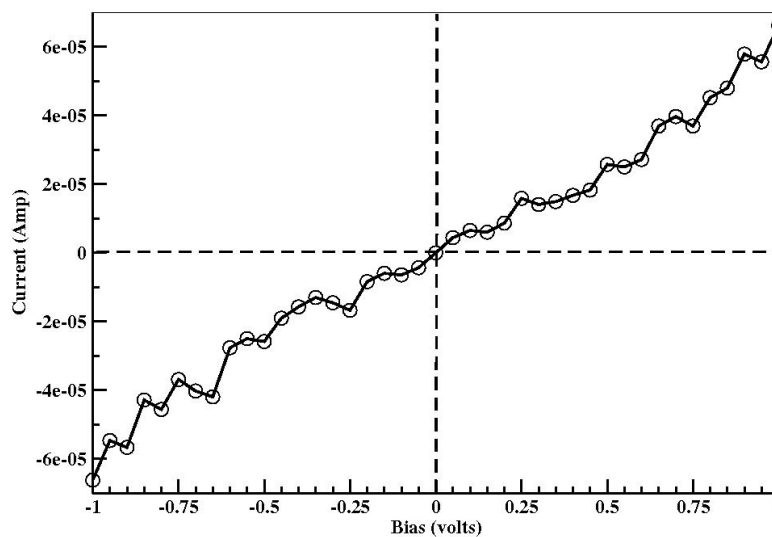


Figure-7

Characteristic Curve I-V of Siznr showing variation of current with applied positive and negative bias

Transmission curve analysis

The behavior of I-V characteristics of SiOznr and siznr mentioned in last section can be explained on the basis of their transmission curves. Electron transport characteristics for silicon mono oxide and silicene in the presence of an external biasing voltage have been studied. As mentioned earlier basis sets comprised of LCAO (linear combination of numerical type atomic orbitals) and k-point sampling chosen for the realistic modeling of the electrode in this study. Present study involves the NEGF method to describe the electronic structure of silicon mono oxide nanoribbon systems composed of two electrode parts and a scattering region.

The transmission spectra at $V = 0.0 \text{ V}, \pm 0.25 \text{ V}, \pm 0.50 \text{ V}, \pm 0.75 \text{ V}, \pm 1.0 \text{ V}$ is shown in Figure-8 (a & b) and Figure-9. We start from the case of zero bias. A sharp peak is observed above Fermi level (E_F) at 1.2 eV and a adjacent peak at 0.8 eV. Below Fermi level (E_F) a sharp peak at 0.8 V is seen. At 0.25 V a peak exists in the bias window which is responsible for current flow. At 0.50 V a peak below Fermi level and tail of peak in the region above Fermi level is responsible for current flow. At 0.75 V two peaks are observed in the bias window and they are contributing for current flow. At 1.0 V a broad peak is observed around Fermi level in the bias window. Thus it is observed that as the bias voltage increases the current flow also increases. At

bias voltage of -0.25 V main contribution to current is made by tail of the peak below Fermi level. As the bias voltage is increased to -0.50 V the current flow is due to a sharp peak below Fermi level and tail of peak which lies in the bias window above Fermi level. Similarly at -0.75 V two peaks lie in the bias window. One is below the Fermi level and the other is above Fermi level which contributes to current. At -1.0 V again two peaks are observed which are responsible for current flow. It is observed that as the negative bias is increased the height of peaks observed above and below the Fermi level decreases.

Analysis of DOS Curve

The DOS curve of silicon nanoribbon with a definite band gap shows semi metallic properties. The conduction bands on right side and valence band on left side of DOS curve become wider

as the bias voltage increases. It is due to the fact that polarization produces a relative displacement of the electrodes energy bands. If Fermi level lies in anti-bonding state (HOMO region) of DOS curve the system will be unstable and not all the bonding states are completely filled necessitating additional electrons to make the system more stable¹⁸ to minimize energy by going into some other configuration.

If we compare DOS curves of SiOznr, shown in Figure-10 with corresponding Transmission curves a sharp peak is observed below Fermi level at 0.0V. The peaks observed at 0.25V, 0.50V, 0.75 V and 1.0 V are almost similar to those observed in transmission curve. As the bias voltage is increased the peak height is decreasing.

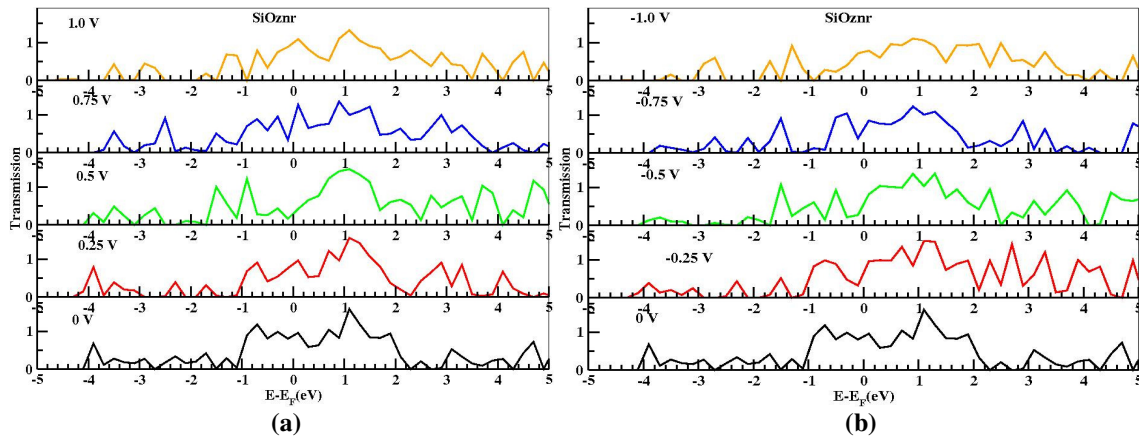


Figure-8
 Transmission curve of SiOznr at different (a) positive bias and (b) negative bias (Color online)

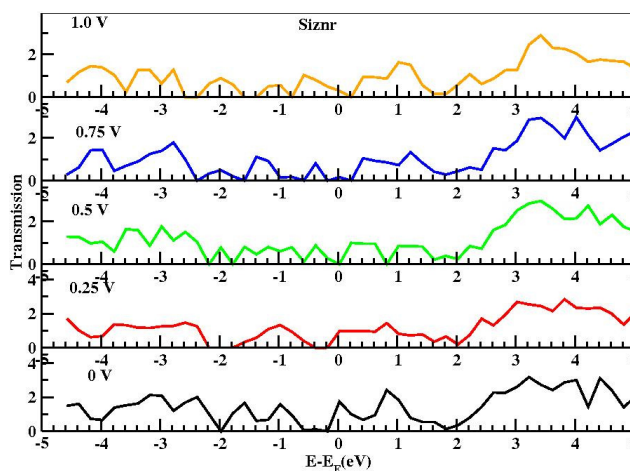


Figure-9
 Transmission curve of Siznr at different positive voltages (similar transmission behavior is shown in negative biasing) (Color online)

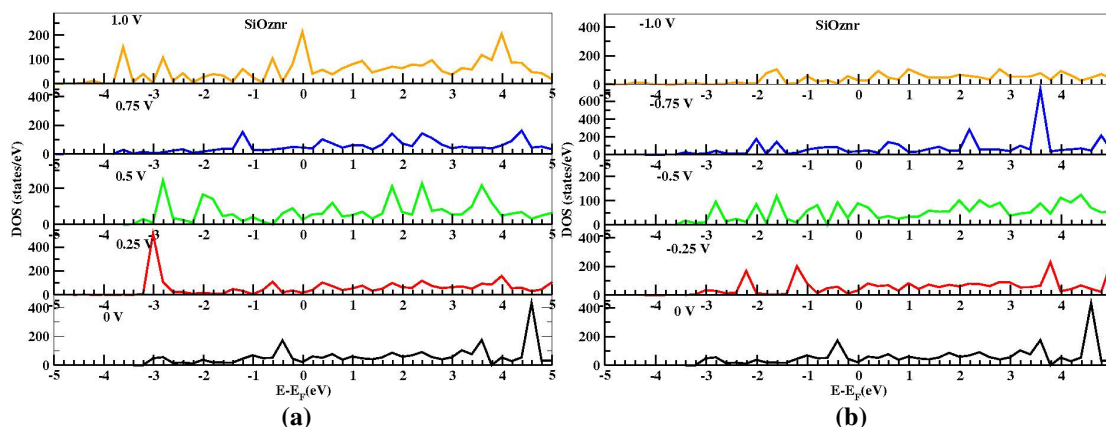


Figure-10

DOS curve of SiOznr at different (a) positive voltages and (b) negative voltages (Color online)

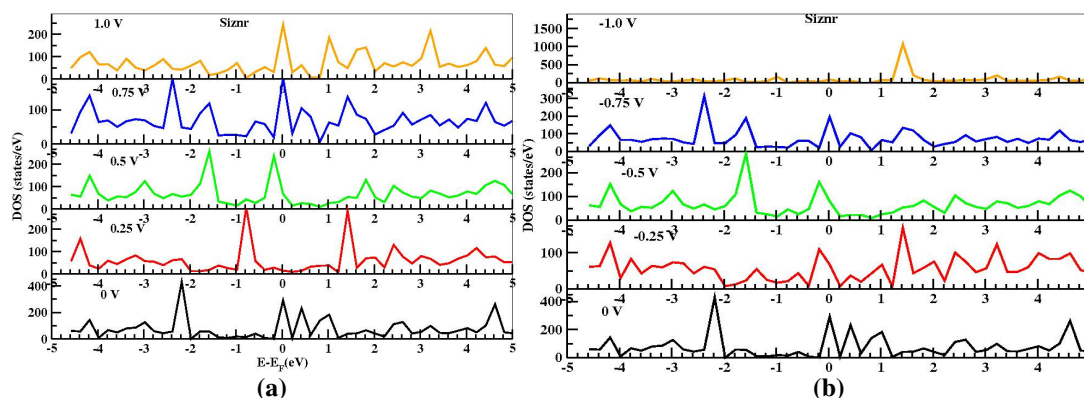


Figure-11

DOS curve of Siznr at different (a) positive voltages and (b) negative voltages (Color online)

In Figure-11, DOS curves of Siznr shows sharp peaks in HOMO region. Also at biasing voltage of 0.75V and 1.0 V a sharp peak is observed in the fermi region. This is attributed to the fact that when applied bias increases the band gap conduction starts. Similar feature is observed with negative bias and reverse current flows.

Conclusion

We have studied transport properties of zigzag SiO nanoribbon within the framework of density functional theory and non equilibrium Greens function formalism. The present first principle study shows that out of the two configurations silicon nanoribbon is having conducting nature. I-V characteristic of SiOznr resembles diode characteristic. The I-V characteristics were well supported by transmission and DOS spectra. The two spectra are strongly correlated, especially in the location of their peaks. For both the systems, there exists a HLG i.e. HOMO (highest occupied molecular orbital)-LUMO (lowest unoccupied molecular orbital) gap. The gap in the transmission spectra can be attributed to the intrinsic semiconducting nature. As revealed from the DOS curves Siznr is showing metallic characteristic. Also it has been reported that Si-O bond length has 50% ionic

character¹⁹. Moreover, in silicon the stability is attained through puckering as reported by S. Cahangirov et al²⁰. Although lot of studies has been reported on SiO₂ nanoparticles and Si nanoribbons but here first attempt has been made to study transport phenomenon in silicon monoxide nanoribbon. It is purely a theoretical work, which may be useful for designing new nanoribbon predicting its properties for different device applications. The successful use of first principle study in the rational design of nanoribbons and their structural and transport properties studies would be an aid to the field of optoelectronics, nanoelectronics.

Recently SnO₂ doped reduced graphene oxide nanoribbons are experimentally studied for a better electrode of Li ion conducting batteries²¹, so similar behaviors useful in different electrochemical devices may be expected for SiO nanoribbons. The detail studies are under progress in our lab.

Acknowledgment

The authors would solemnly like to acknowledge their gratitude to the management of Shri Shankaracharya Group of Institutions (SSTC) for their kind support and to the Principal of UPU

Government Polytechnic, Durg. Helpful discussions with Prof. Ravindra Pandey, Fellow of American Physical Society, Michigan Technological University, USA is acknowledged.

References

1. Cahangirov S., Topsakal M., Akturk E., Şahin H. and Ciraci S. (2009). Two-and one-dimensional honeycomb structures of silicon and germanium. *Phys. Rev. Lett.*, **102**, 236804.
2. Zhang Y., Yan-Wen Tan, Stormer H.L. and Kim P. (2005). Experimental observation of the quantum Hall effect and Berry's phase in graphene. *Nature London*, 438, 201-4.
3. Takeda K. and Shiraishi K. (1994). Theoretical possibility of stage corrugation in Si and Ge analogs of graphite. *Phys. Rev.*, B **50**, 14916.
4. Durgun E., Tongay S. and Ciraci S. (2005). Silicon and III-V compound nanotubes: Structural and electronic properties. *Phys. Rev.*, B **72**, 075420.
5. Cho Ko Heung, Baca Alfred J. and A. Rogers Bulk John (2006). Quantities of Single-Crystal Silicon Micro-/Nanoribbons Generated from Bulk Wafers. *Nano letters*, 6(10), 2318-2324.
6. www.uam.es/siesta.
7. Perdew J.P. and Ernzerhof K.M. (1996). Generalized Gradient Approximation Made Simple. *Phys. Rev. Lett.*, **77** 3865-3868.
8. Jaffe J.E., Snyder J.A., Lin Z. and Hess A.C. (2000). LDA and GGA calculations for high-pressure phase transitions in ZnO and MgO. *Phys. Rev.*, B **62**, 1660-1665.
9. Zhu X. and Louie S.G. (1991). Quasiparticle band structure of thirteen semiconductors and insulators. *Phys. Rev.*, B **43**, 14142.
10. Li Z.Y. and Daniel S.K. (2006). Dithiocarbamate anchoring in molecular wire junctions: a first principles study. *J Phys Chem B*, 110 (20), 9893-9898.
11. Trivedi S., Srivastava A. and Kurchania R. (2013). Electronic and transport properties of Silicene nanoribbon. *J Comput Theor Nanosci*, 11, 789-794.
12. Srivastava Anurag, Jain Sumit Kumar and Khare Purnima Swarup (2014). Ab-initio study of structural, electronic, and transport properties of zigzag GaP nanotubes. *J Mol Model*, 20, 2171.
13. Brandbyge M., Mozos J.L., Ordejón, Taylor J. and Stokbro K. (2002). Density-functional method for nonequilibrium electron transport. *Phys. Rev. B*, 65, 165401 1-17.
14. Şahin H., Cahangirov S., Topsakal M., Bekaroglu E., Akturk E., Senger R.T. and Ciraci S. (2009). Monolayer honeycomb structures of group-IV elements and III-V binary compounds: First-principles calculations. *Physical Review*, B **80**, 155453.
15. Reed M.A., Chen J., Rawlett A.M., Price D.W. and Tour J.M. (2001). Molecular Random Access Memories. *App. Phys. Lett.*, **78**, 3735-3737.
16. Husband C.P., Husband S.M., Daniels J.S. and Tour J.M. (2003). Logic and Memory with Nanocell Circuits. *IEEE T. on Electron Dev.*, **50**, 1865-1975.
17. Quek S.Y., Neaton J.B., Hybertsen M.S., Kaxiras E. and Louie S.G. (2007). Negative Differential Resistance in Transport through Organic Molecules on Silicon. *Phys. Rev. Lett.*, **98**, 066807.
18. Gibbs G.V., Hamil M.M. and Louisnathan S.J. (1972). Correlations between si-o bond length, si-o-si angle and bond overlap populations calculated using extended huckel molecular orbital theory. *American Mineralogist*, **57**, 1578-1613.
19. Ravindran P. and Asokamani R. (1997). Correlation between electronic structure, mechanical properties and phase stability in intermetallic compounds. *Bull. Mat. Sci.*, **20**(4), 613-622.
20. Cahangirov S., Topsakal M., Akturk E., Şahin H. and Ciraci S. (2009). Two-and one-dimensional honeycomb structures of silicon and germanium. *Phys. Rev. Lett.*, **102**, 236804.
21. Lei Li, Anton Kovalchuk, and James M. Tour (2014). SnO₂-reduced graphene oxide nanoribbons as anodes for lithium ion batteries with enhanced cycling stability. *Nano Research*, 7(9), 1319-1326.